Dynamics of solitons and quasisolitons of the cubic third-order nonlinear Schrödinger equation

V. I. Karpman,[1] J. J. Rasmussen,[2] and A. G. Shagalov[3]

[1]*Racah Institute of Physics, Hebrew University of Jerusalem, Jerusalem 91904, Israel*
[2]*Department of Optics and Fluid Dynamics, Risoe National Laboratory, Box 49, DK-4000 Roskilde, Denmark*
[3]*Institute of Metal Physics, Ekaterinburg 620219, Russia*

The dynamics of soliton and quasisoliton solutions of the cubic third-order nonlinear Schrödinger equation is studied. Regular solitons exist due to a balance between the nonlinear terms and (linear) third-order dispersion; they are not important at small α_3 (α_3 is the coefficient in the third derivative term) and vanish at $\alpha_3 \rightarrow 0$. The most essential, at small α_3, is a quasisoliton emitting resonant radiation (resonantly radiating soliton). Its relationship with the other (steady) quasisoliton, called embedded soliton, is studied analytically and also in numerical experiments. It is demonstrated that the resonantly radiating solitons emerge in the course of nonlinear evolution, which shows their physical significance.

I. INTRODUCTION

Equations describing soliton processes are usually obtained by certain approximating procedures affecting nonlinearity and dispersion. Now, in extensive studies of ultrafast processes, the classical approximations often appear to be insufficient and higher-order effects become of importance. A typical example is high speed systems like nonlinear transmission lines in the femtosecond regime for soliton communications, etc. For such systems soliton solutions in classical sense do not generally exist. Only for very specific choices of parameters one can find localized solutions. Instead of regular solitons there may appear nonlocal steady or (and) unsteady solitonlike structures (which may be called quasisolitons). These may, however, have significant importance for the nonlinear dynamics.

In this paper we study wave dynamics described by the extended third-order cubic nonlinear Schrödinger (NLS) equation

$$i\partial_T\Psi + \frac{1}{2}\partial_X^2\Psi + |\Psi|^2\Psi + i\alpha_1|\Psi|^2\partial_X\Psi + i\alpha_2\Psi\partial_X|\Psi|^2$$

$$+ i\alpha_3\partial_X^3\Psi = 0 \qquad (1)$$

[with real coefficients $\alpha_n (1 \leq n \leq 3)$]. This equation describes, in general, the slow evolution of the wave envelope in nonlinear highly dispersive systems. It plays an important role in many nonlinear problems, in particular, in nonlinear fiber optics [1,2]. In that connection T denotes the distance along the fiber, while X is related to the retarded time. The second term describes the group velocity dispersion (which we have chosen to be anomalous in the present case), the third term designates the self-phase modulation (related to the nonlinear frequency shift), the fourth term relates to the self-steepening effects, the fifth term is so-called Raman term relating to the self-frequency shift, and the sixth term describes the third-order dispersion effect. Equation (1) reduces to the standard cubic NLS equation for $\alpha_1 = \alpha_2 = \alpha_3 = 0$, which is integrable. The "extra" terms become of importance for ultrashort (e.g., in femtosecond range) pulses.

Equation (1) has regular soliton solutions [3–5], vanishing at $|X| \rightarrow 0$. In particular cases, Eq. (1) may have exact N soliton solutions [4] or even be integrable [5]. An important feature of the solutions describing regular solitons is that they are degenerating at $\alpha_3 \rightarrow 0$ (and finite $|\alpha_1| + |\alpha_2|$), which substantially reduces their physical importance. Their numerical investigation at $\alpha_{1,2} \sim \alpha_3 \sim 1$ where done, e.g., in Ref. [6] (see also references therein)

There also exist some solutions to Eq. (1), describing quasisolitons. One of them is a steady solution looking like a soliton-type pulse embedded into a small amplitude plane wave (a soliton on plane wave pedestal). We call it *embedded* soliton (ES), using the word proposed in a different context in Ref. [7]. Apart from that, Eq. (1) has other types of quasisoliton solutions that describe solitonlike pulses permanently emitting resonantly generated radiation [see, e.g., Refs. [8–12] for the particular case at $\alpha_1 = \alpha_2 = 0$ and [13,14] for the full Eq. (1)]. We will call them resonantly radiating solitons (RRS); they are unsteady because of losses caused by the radiation. The lifetime of radiating soliton is sufficiently large if α_3 is small enough and, naturally, one can speak about the soliton only in this quasisteady case. (However, at long times, the losses caused by the radiation become essential for applications [2].) At $\alpha_3 \rightarrow 0$, the RRS turns into the regular soliton of Eq. (1) without the third derivative.

There is an interesting and important connection between the two types of quasisolitons, ES and RRS, and we demonstrate it in numerical simulations. We will also study the role of solitons and quasisolitons in the nonlinear processes described by Eq. (1). In particular, the regular solitons and RRS compete between themselves in nonlinear processes. As far as the regular solitons disappear at $\alpha_3 \rightarrow 0$ and the RRS have short lifetimes at large α_3, it is clear that at large α_3 the regular solitons are more important while the RRS may play a decisive role at sufficiently small α_3. The most interesting case is, of course, small α_3, because the third derivative term emerges as the result of an expansion. (The effect of next, fourth derivative, term can be seen in Refs. [13,14]; at certain relationship between the coefficients before third and

fourth derivatives there can be no radiation at all which, naturally, may happen also when other high-order terms are taken into account.)

The paper is organized as follows. In Sec. I we describe important properties of Eq. (1), which are used below. In particular, we discuss regular soliton solutions [3], Galilean transformations and conservation laws [13,14]. The embedded solitons are studied in Sec. III. As we have already mentioned, the ES consists of a steady solitonlike pulse on the plane wave background. This structure is rather common in different nonlinear highly dispersive systems [9–20]. At $\alpha_3 \rightarrow 0$, the plane wave disappears and the pulse turns into a regular soliton of Eq. (1) at $\alpha_3 = 0$. The plane wave amplitude, increasing with α_3, may become unstable at sufficiently large α_3 due to the modulational instability. Considering small α_3, we show that the pulse part of ES is rather close to the pulse in RRS and the wave number of the plane wave coincides with the wave number of resonantly emitted radiation (by the RRS). Next, we introduce the *cutoff* operation, cutting off both wave wings from the ES (Sec. IV). Then we see that the remained solitonlike pulse is transformed into the RRS, emitting radiation only in *one direction*, according to the direction of the group velocity of resonant radiation. The resonant radiation disappears at $\alpha_1 = 6\alpha_3$. In this case, considered in Sec. V, we show that Eq. (1) can be transformed, by means of the Galilean transformation, to the complex modified Korteweg-de Vries (MKdV) equation. At particular initial conditions, it is reduced to the real MKdV equation, which is integrable and therefore has N-soliton solutions [22]. This does not mean the complete integrability of Eq. (1) at $\alpha_1 = 6\alpha_3$, because the reduction to the real MKdV equation is possible only for particular initial conditions. On the other hand the Painlevé analysis [21] of the above mentioned *complex* MKdV equation shows that it possesses the Painlevé property at $6\alpha_3 = \alpha_1 = 2\alpha_2$. This is just the case when Eq. (1) is integrable [5]. If $\alpha_2 = 0$, we arrive at the case considered by Hirota [4] who has shown the existence of complex N-soliton solutions. In Sec. VI, we consider the case $\alpha_1 \neq 6\alpha_3$. Solving numerically the initial value problem, we show that, at sufficiently small α_3, the initial disturbances decay into RRS. This indicates that the RRS are important physical objects playing a significant role in nonlinear dynamics. In Sec. VII, a summary of obtained results is given. In Appendix A, the modulational instability of a plane wave, described by Eq. (1), is considered; it is helpful in the study of the stability of embedded solitons. In Appendix B we investigate analytically, by means of conservation laws, the evolution of RRS caused by the radiation. This analysis is in agreement with numerical results described in Secs. IV and VI.

II. IMPORTANT PROPERTIES OF EQ. (1)

A. Exact soliton solutions

First, we discuss the exact soliton solutions of Eq. (1). They can be written in the form

$$\Psi_s = a \, \text{sech}[b(X - V_s T)]e^{i\kappa X - i\omega T}, \tag{2a}$$

$$a^2 = \frac{6\alpha_3}{\alpha_1 + 2\alpha_2}b^2 \quad (\alpha^2 > 0), \tag{2b}$$

$$V_s = \kappa - 3\alpha_3\kappa^2 + \alpha_3 b^2, \tag{2c}$$

$$\omega = \frac{1}{2}\kappa^2 - \alpha_3\kappa^3 - \frac{1 - 6\alpha_3\kappa}{2}b^2, \tag{2d}$$

$$\kappa = \frac{\alpha_1 + 2\alpha_2 - 6\alpha_3}{12\alpha_2\alpha_3}. \tag{2e}$$

In fact, these are the soliton solutions found by Potasek and Tabor [3] (with corrected misprints). We will call Eqs. (2a–e) Potasek-Tabor (PT) soliton solutions. At $\alpha_3 = 0$, PT solitons do not exist; this signifies that their existence is a result of a balance between the nonlinear terms and the linear third-order dispersive term. If $\alpha_2 \neq 0$, from Eq. (2e) it follows that κ is a fixed number, uniquely determined by the coefficients of Eq. (1). However, the solitons (2) exist even at $\alpha_2 = 0$ provided that

$$\alpha_1 = 6\alpha_3. \tag{3}$$

In this case κ can be *arbitrary*, because Eq. (2e) follows from the equation $12\alpha_2\alpha_3\kappa = \alpha_1 - 6\alpha_3 + 2\alpha_2$.

In case (3) and $\alpha_2 = 0$, Eq. (1) is the so called Hirota equation that can be transformed to the complex modified Korteweg-de Vries equation, which has N-soliton solutions [4]. For the Hirota soliton, from Eq. (2b) it follows

$$b = a. \tag{4}$$

In the other particular case, $6\alpha_3 = \alpha_1 = 2\alpha_2$, Eq. (1) is integrable [5]. (See also Sec. V.) Some results for solitons (2) with $\alpha_2 \neq 0$ were reported in Ref. [6] (see also references therein). In particular, it was shown numerically that they emerge in a solution of the initial value problem. However, this result was obtained at $\alpha_1 = \alpha_3 = 1$; at small α_3, as it will be shown below, they cannot compete with RRS.

Apart from the solution (2a–e), describing "bright" solitons, which was called in Ref. [3] sech family, Potasek and Tabor have also found tanh family that will not be discussed here. (Some generalizations, with both sech and tanh terms, are derived in Ref. [27] by means of rather tedious algebra; the results of this paper are mostly contained in Ref. [3], and the generalizations [27], which are valid for very specific choices of the parameters, can be obtained by the much simpler approach of Potasek and Tabor.) The results of Ref. [3] are repeated also in some other papers (e.g., [23]).

B. Galilean transformation

In the following we shall frequently use the Galilean transformation describing the transition to the reference frame moving with the velocity V. For Eq. (1) it reads

$$\Psi(X, T) = \psi(X - VT, T)\exp[i(KX - \Omega T)], \tag{5}$$

where K and Ω are defined by equations

$$V = K - 3\alpha_3 K^2, \tag{6}$$

$$\Omega = \frac{1}{2}K^2 - \alpha_3 K^3. \tag{7}$$

The function $\psi(x,t)$ with

$$x = X - VT, \quad t = T \tag{8}$$

satisfies the equation [13,14]

$$i\partial_t \psi + \frac{1}{2}a_2\partial_x^2\psi + q|\psi|^2\psi + i\alpha_1|\psi|^2\partial_x\Psi + i\alpha_2\psi\partial_x|\psi|^2$$

$$+ i\alpha_3\partial_x^3\psi = 0, \tag{9}$$

with

$$a_2 = 1 - 6\alpha_3 K, \tag{10}$$

$$q = 1 - \alpha_1 K. \tag{11}$$

C. Conservation laws

One can check by means of straightforward calculations that Eq. (1) has the following integral of motion

$$N = \int_{-\infty}^{\infty} |\Psi(X,T)|^2 dX. \tag{12}$$

At

$$\alpha_2 = 0, \tag{13}$$

we have two other conserved integrals [24,13,14]

$$P = \frac{1}{2}i\int_{-\infty}^{\infty}(\Psi\partial_X\Psi^* - \Psi^*\partial_X\Psi)dX, \tag{14}$$

$$H = \int_{-\infty}^{\infty}\left\{\frac{1}{2}|\partial_X\Psi|^2 - \frac{1}{2}|\Psi|^4 - \frac{1}{4}i\alpha_1|\Psi|^2(\Psi^*\partial_X\Psi\right.$$

$$\left. - \Psi\partial_X\Psi^*) - \frac{1}{2}i\alpha_3(\Psi^*\partial_X^3\Psi - \Psi\partial_X^3\Psi^*)\right\}dX. \tag{15}$$

III. EMBEDDED SOLITONS

We start with the solutions to Eq. (1) of the form

$$\Psi(X,T) = \chi(x)e^{i\Lambda t}, \tag{16}$$

where x and t are defined in Eq. (8). Substituting Eq. (16) into Eq. (1), we arrive at the ordinary differential equation

$$-iV\partial_x\chi + \frac{1}{2}\partial_x^2\chi + |\chi|^2\chi + i\alpha_1|\chi|^2\partial_x\chi + i\alpha_2\chi\partial_x|\chi|^2$$
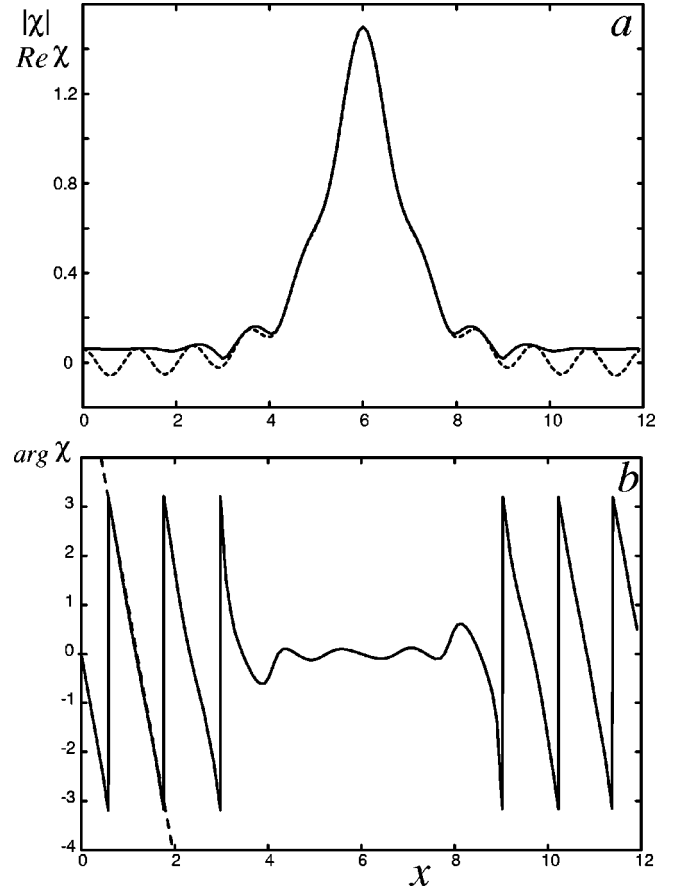
$$+ i\alpha_3\partial_x^3\chi = \Lambda\chi. \tag{17}$$

FIG. 1. Numerical solution of Eq. (17) at parameters (18). (a) χ versus x; solid line: $|\chi(x)| = |\Psi(x)|$; dashed line: Re $\chi(x)$. (b) arg χ versus x; at sufficiently large $|x-x_0|$, arg $\chi(x)$ is a linear function: arg $\chi \approx \kappa|x-x_0|$, which permits to measure κ ($\kappa \approx -5.2$).

Imposing periodic boundary conditions at the ends of a sufficiently broad interval and considering V and $\chi(0)$ as given parameters and Λ as the eigenvalue, we arrive at a nonlinear eigenvalue problem that can be numerically solved by a kind of shooting method. An example of such solution at $\alpha_2 = 0$ and

$$\alpha_1 = -0.3, \quad \alpha_3 = -0.1, \quad \chi(0) = 1.5, \quad V = 0 \tag{18}$$

is shown in Figs. 1(a) and 1(b). It is a nonlocal steady pulse with $|\Psi(x)|_{max} = |\Psi(x_0)|$ and small symmetric "wings." At large $|x-x_0|$ we can linearize Eq. (17); then we see that

$$\chi(x) \approx \text{const } e^{i\kappa x} \quad (|x-x_0| \gg 1), \tag{19}$$

where κ is a real root of the cubic algebraic equation

$$\Lambda - \kappa V + (1/2)\kappa^2 - \alpha_3\kappa^3 = 0. \tag{20}$$

Finding Λ from the numerical solution of the eigenvalue problem and κ from Eq. (20), we have for the case (18)

$$\Lambda = 0.979, \quad \kappa = -5.34. \tag{21}$$

On the other hand, we can determine κ directly from $\chi(x)$ that is found numerically from Eq. (17), together with Λ.

From Fig. 1(b) we see that the numerically found $\chi(x)$ has indeed the asymptotic behavior (19) with $\kappa \approx -5.3$ that is very close to the root of Eq. (20), written in Eq. (21). This agreement is an evidence of the correctness of the numerical solution of the eigenvalue problem by the shooting method. In a similar way, the solution of eigenvalue problem (17) and Eq. (20) for $\alpha_2 = 0$ and

$$\alpha_1 = -0.8, \quad \alpha_3 = -0.1, \quad \chi(0) = 1.5, \quad V = -0.225 \tag{22a}$$

gives

$$\Lambda = 1.209, \quad \kappa = -5.03. \tag{22b}$$

The asymptotic behavior of the numerically found $\chi(x)$ gives the same $\kappa \approx -5.03$.

For the other case with $\alpha_2 = 0$ and

$$\alpha_1 = -1.1, \quad \alpha_3 = -0.1, \quad \chi(0) = 1.5, \quad V = 0.35 \tag{23a}$$

we have

$$\Lambda = 1.937, \quad \kappa = -6.12, \tag{23b}$$

while from the numerically found $\chi(x)$ we obtain $\kappa = -6.1$.

In fact, similar quasisoliton solutions, looking like embedded solitons, were obtained, by different approaches, for other highly dispersive systems as well [15–17,9,11,12,18–20].

Now consider the embedded solitons, starting from the Galilean transformation (5). Writing it in the form

$$\Psi(X,T) = \psi(x,t) e^{iKx} \exp[i(KV - \Omega)t] \tag{24}$$

and assuming that

$$\psi(x,t) = \tilde{\psi}(x) \exp\left(i\frac{1}{2}\lambda^2 t \right), \tag{25}$$

where λ is a constant parameter, we compare Eq. (24) with Eq. (16). Then we have

$$\tilde{\psi}(x) = \chi(x) \exp(-iKx), \tag{26}$$

$$\lambda^2 = 2(\Lambda + \Omega - KV). \tag{27}$$

From Eqs. (25) and (9) we arrive at the following equation for $\tilde{\psi}(x)$

$$-\frac{1}{2}\lambda^2\tilde{\psi} + \frac{1}{2}a_2\partial_x^2\tilde{\psi} + q|\tilde{\psi}|^2\tilde{\psi} + i\alpha_1|\tilde{\psi}|^2\partial_x\tilde{\psi} + i\alpha_2\tilde{\psi}\partial_x|\tilde{\psi}|^2$$
$$+ i\alpha_3\partial_x^3\tilde{\psi} = 0, \tag{28}$$

Substituting here Eqs. (26) and (27) and taking into account Eqs. (6) and (7) and Eqs. (10) and (11) we have Eq. (17) as one should expect. From Eq. (26) it is seen that $|\tilde{\psi}|^2 \ll 1$ at $|x| \gg 1$. Linearizing Eq. (28) we obtain

$$\tilde{\psi} \sim e^{ikx} \quad (|x| \gg 1), \tag{29}$$

where k is a root of the equation

$$2\alpha_3 k^3 - a_2 k^2 - \lambda^2 = 0. \tag{30}$$

Substituting Eqs. (19) and (29) into Eq. (26), we see that

$$\kappa = k + K. \tag{31}$$

Then, using Eqs. (6) and (7) and Eqs. (10) and (27) we can easily prove that Eqs. (30) and (20) are equivalent, as it should be.

At small α_3, the solution of Eq. (28) can be written as

$$\tilde{\psi}(x) = [u_s(x) + f(x)] \exp[i\phi_s(x)], \tag{32}$$

with small $f(x)$. Here $u_s(x)$ and $\phi_s(x)$ are defined by the requirement that

$$F(x) = u_s(x) \exp[i\phi_s(x)] \tag{33}$$

is a soliton solution of Eq. (28) without the last term i.e.,

$$-\frac{1}{2}\lambda^2 F + \frac{1}{2}a_2\partial_x^2 F + q|F|^2 F + i\alpha_1|F|^2\partial_x F + i\alpha_2 F\partial_x|F|^2 = 0 \tag{34}$$

and $F(x) \to 0$ at $x = \pm\infty$. Solving Eq. (34), we have

$$u_s(x) = \lambda \sqrt{\frac{2p}{q}} \left[\cosh\left(\frac{2\lambda}{\sqrt{a_2}} x \right) + p \right]^{-1/2}, \tag{35}$$

$$\phi_s(x) = -\frac{\alpha_1 + 2\alpha_2}{2A} \arctan\left[\sqrt{\frac{1-p}{1+p}} \tanh\left(\frac{\lambda x}{\sqrt{a_2}} \right) \right], \tag{36}$$

$$p = \frac{\sqrt{a_2}q}{\sqrt{4A^2\lambda^2 + a_2 q^2}}, \tag{37}$$

$$A^2 = \frac{4\alpha_1(\alpha_1 + 2\alpha_2) - (\alpha_1 + 2\alpha_2)^2}{12}. \tag{38}$$

Equations (35)–(38) were obtained in Ref. [14] for a pulse part of RRS. From Eq. (35) it follows that the soliton amplitude is

$$u_0 = \lambda \sqrt{\frac{2p}{(1+p)q}} \tag{39}$$

and its width is given by

$$\delta = \sqrt{a_2}/\lambda. \tag{40}$$

Thus one must require $a_2 > 0$ and from Eq. (10) it follows that at $\alpha_3 K > 0$,

$$|K| < \frac{1}{6}|\alpha_3|, \tag{41}$$

which is a restriction on the soliton velocity (6).

The small term $f(x)$ in Eq. (32) expresses the effect of the third-order dispersion. At $|x| \sim \sqrt{(a_2)}/\lambda$, or less, it describes the modification of the pulse, arising due to the last term in Eq. (28), while at large x

$$f(x) \approx \widetilde{\psi}(x) \sim e^{ikx} \tag{42}$$

where k is a root of Eq. (30). Note, that this equation was derived in Ref. [14] for the wave number of the resonantly generated radiation by the RRS in the reference frame where the RRS is at rest. From all that we conclude that Eq. (32) coincides with the asymptotic expression for the RRS and its radiation at large t.

Let us now compare the embedded solitons, obtained above numerically, with the solution (32) at condition (13). From Eq. (38) we have

$$A = \frac{1}{2} |\alpha_1|. \tag{43}$$

Equations (6) and (10) give

$$K = \frac{1 - \sqrt{1 - 12\alpha_3 V}}{6\alpha_3}, \tag{44}$$

$$a_2 = \sqrt{1 - 12\alpha_3 V}. \tag{45}$$

Using Eqs. (39) and (37), we obtain

$$u_0^2 = \frac{\sqrt{a_2}}{2A^2} (\sqrt{4A^2\lambda^2 + q^2 a_2} - q\sqrt{a_2}), \tag{46}$$

where q is defined in Eq. (11). From Eq. (27) and Eqs. (6) and (7) we find

$$\lambda^2 = 2\left(\Lambda - \frac{1}{2}K^2 + 2\alpha_3 K^3\right). \tag{47}$$

Then we have for the case (18) and (21), which is shown in Fig. 1: $u_0 \approx 1.37$. For the case (22) $u_0 \approx 1.41$, and for case (23) $u_0 \approx 1.42$. So, in all three cases we approximately have $u_0 \approx 1.4$ which is rather close to $\chi(0) = 1.5$, assumed in the nonlinear eigenvalue problem for all three cases. This supports the conclusion that expressions (35) and (36) approximately describe the pulse in the embedded soliton (at small α_3).

Now consider $f(x)$. At small α_3, the roots of Eq. (30) have simple analytical expressions [14]. Neglecting the first term in Eq. (30), we have the two smallest roots

$$k \approx \pm i \frac{\lambda}{\sqrt{a_2}}. \tag{48}$$

Substituting this into Eq. (42), we have

$$\widetilde{\psi} \approx f(x) \sim \exp(\mp \lambda/\sqrt{a_2}x). \tag{49}$$

This is in agreement with the asymptotic behavior of expression (33) at large x. The third root can be approximately obtained if one neglects the last term in Eq. (30). This gives

$$k \approx a_2/2\alpha_3, \tag{50}$$

which approximately determines the wave number of the plane wave in the wings. Expressions (50) and (31) approximately give the roots of Eq. (20) in analytical form. From Eq. (50) it follows

$$\mathrm{sgn}\, k = \mathrm{sgn}\, \alpha_3. \tag{51}$$

And, finally, from the results of Ref. [14] it follows that at small α_3

$$f(x) \approx B\left(\frac{\sqrt{a_2}|k|}{A}\right)^{1/2} \exp\left[-\frac{\pi\sqrt{a_2}|k|}{4\lambda}\left(1 + \frac{2}{\pi}\arcsin p\right)\right] e^{ikx}, \tag{52}$$

where B is a complex constant with $|B| \sim 1 - 10$. This expression is valid at

$$\frac{\sqrt{a_2}|k|}{\lambda} \gg 1, \tag{53}$$

i.e., when the wave number k is much larger than the inverse width of the soliton (33). In expression (52), it is also assumed that $2A\lambda \gg \lambda/\sqrt{a_2}|k_{1,2}|$ (this does not exclude $A\lambda \ll 1$). If

$$2A\lambda \sim \lambda/\sqrt{A_2}|k_{1,2}| \quad (\text{or } 2A\lambda < \lambda/\sqrt{a_2}|k_{1,2}|), \tag{54}$$

which may be satisfied only at $p \approx 1$ and $q \approx 1$, we have

$$f(x) = B\sqrt{a_2}|k|\exp\left(-\frac{\pi\sqrt{a_2}|k|}{2\lambda}\right) e^{ikx}. \tag{55}$$

It is easy to check that we can arrive at Eq. (55) by substituting in Eq. (52) the first of conditions (54) and $p = 1$.

From all the foregoing, one can see a connection between the embedded and resonantly radiating solitons. In the next section we present numerical experiments disclosing this connection from another side.

IV. THE CUTOFF OPERATION

Let us define a cutoff operation transforming the embedded soliton into an isolated pulse. Turning to the function $\chi(x)$ in Eq. (16), we write

$$\chi_{cut}(x) = \chi(x) r(x), \tag{56}$$

where $r(x)$ is a cutting factor that we take in the form

$$r(x) = \frac{1}{2}\left[\tanh\left(\frac{x - x_0 + \Delta x}{\gamma}\right) - \tanh\left(\frac{x - x_0 - \Delta x}{\gamma}\right)\right]. \tag{57}$$

Here x_0 is the center of the pulse and $\Delta x > 0$ is the width of the cutted function $\chi_{cut}(x)$. According to Eq. (57), $r(x)$ vanishes at $|x - x_0| \to \infty$ and the positive parameter γ characterizes the "sharpness" of vanishing. Assuming that γ is small
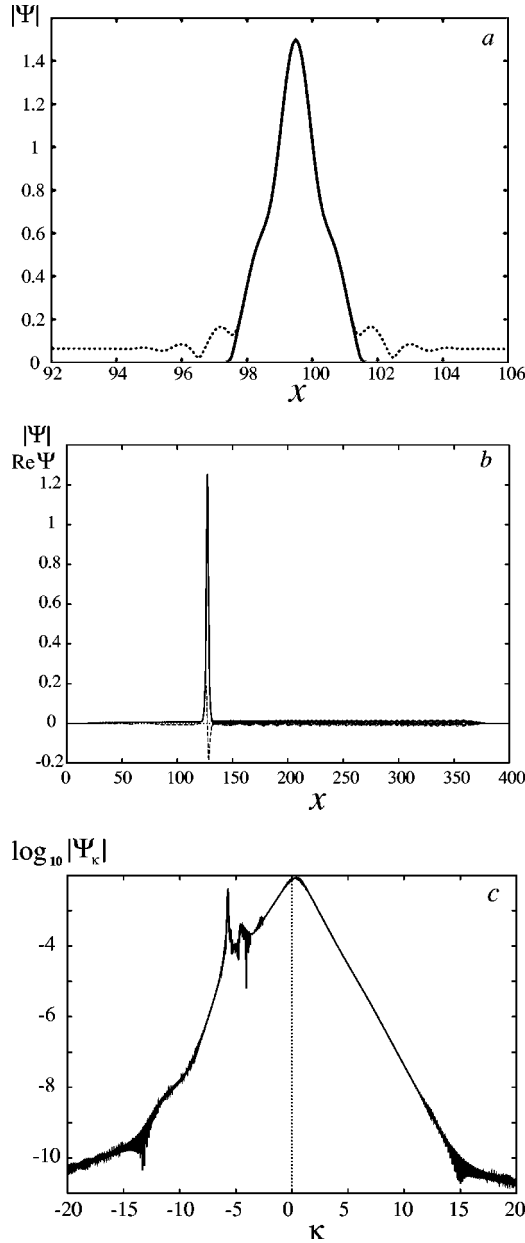
FIG. 2. Numerical solution of Eq. (1) at initial condition (58) and $\alpha_1 = -0.3$, $\alpha_2 = 0$, $\alpha_3 = -0.1$. (a) The initial cut pulse. Full line: $|\Psi|$ versus x at $T = 0$; dotted line depicts the corresponding embedded soliton. (b) The cutoff pulse at $T = 138$; full line: $|\Psi|$ versus x; dashed line: $\text{Re}\,\Psi$ versus x. (c) $\log_{10}|\Psi_\kappa|$ versus κ (Ψ_κ is the Fourier transform of $\Psi(x)$; one can see a peak near the root of resonance equation (20).

enough and Δx is such that the factor $r(x)$ cuts off only the wings without essential disturbing the pulse in $\chi(x)$ (γ and Δx can be properly chosen in numerical tests) we then take the pulse $\chi_{cut}(x)$ as the initial condition to Eq. (1) [see Fig. 2(a)]

$$\Psi(X,0) = \chi_{cut}(X). \tag{58}$$

In Fig. 2(b) one can see that the cutted pulse emits radiation at $t > 0$. However, on the left hand side of the pulse the

radiation spreads out with time; this shows that on the left hand side there is a transient radiation, emitted at small t due to the initial condition (58). On the contrary, on the right hand side we see a wave train with approximately constant amplitude, with the front propagating to the right; so, the length of the wave train increases with time. Therefore the cutoff pulse permanently emits radiation to the right. The spectrum, shown in Fig. 1(c), has a peak at κ approximately equal to the root of Eq. (20) with account of finite velocity of the pulse at $t = 138$ (it is still rather close to κ from Eq. (21), i.e., to the wave number of the wing waves in embedded soliton).

Analyzing the time behavior of $\arg\Psi$, we find that $d(\arg\Psi)/dt = \Lambda(t)$ is a slow function of t, with $\Lambda(0) \approx 0.98$ and $\Lambda(130) \approx 0.85$. Note that this $\Lambda(0)$ coincides, with a good accuracy, with Eq. (21). Similar results were obtained for cutoff pulses in cases (22) and (23).

We conclude that the cutoff pulses are radiating solitons; and the radiation is permanently emitted only in one direction. As far as κ is connected with k from Eq. (31), which is the real root of Eq. (30), obtained from the resonant condition, we conclude that the cutoff operation transforms ES into RRS. The front of radiated wave train propagates with the group velocity $U(k)$ given by [14]

$$U(k) = a_2 k - 3\alpha_3 k^2 \approx -a_2/4\alpha_3. \tag{59}$$

From this it follows that

$$\text{sgn}\,U(k) = -\text{sgn}\,k = -\text{sgn}\,\alpha_3. \tag{60}$$

Therefore at $\alpha_3 < 0$ it should be $k < 0$ and $U(k) > 0$. This means that the soliton in Fig. 2(a) should permanently emit radiation to the right while the peak in the spectrum of the wave train should be at negative k. This is in agreement with the results presented in Figs. 2(b) and 2(c).

To describe analytically the whole system after the cutoff, one can use at small α_3 the equation [14]

$$\tilde{\psi}(x,t) = [u_s(x) + \eta(x,t)]\exp[i\phi_s(x)], \tag{61}$$

where $u_s(x)$ and $\phi_s(x)$ are given (in adiabatic approximation) by Eqs. (35) and (36) and $\eta(x,y)$, at large x and t, has the following asymptotic expression

$$\eta(x,t) \approx f(x)\Theta(Ux)\Theta(|U|t - |x|). \tag{62}$$

Here $f(x)$ is given by Eq. (52) and $\Theta(Y)$ is the Heaviside function

$$\Theta(Y) = 1 \quad (Y > 0), \quad \Theta(Y) = 0 \quad (Y < 0). \tag{63}$$

Equation (62) expresses that the soliton radiates in the direction of group velocity U and the radiation front propagates with the velocity $|U|$. The above mentioned adiabatic approximation means that at sufficiently small α_3, the radiation is so small that the soliton parameters in $u_s(x)$ and $\psi_s(x)$ (as well as the wave number k) can be considered as constant. However, the soliton losses may be essential at large times.

The variation of soliton parameters, caused by the radiation, can be estimated by means of the integrals of motion (Appendix B). A vast information about the soliton evolu-
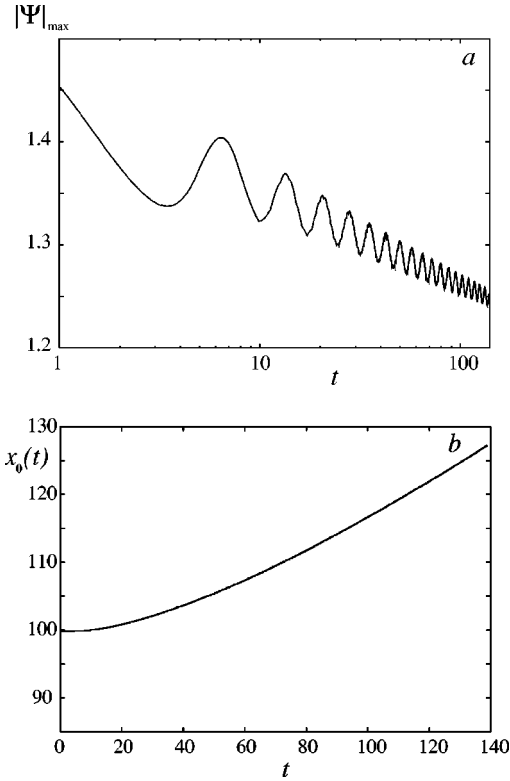
FIG. 3. Temporal behavior of the radiating soliton at $\alpha_1 = -0.3$, $\alpha_2 = 0$, $\alpha_3 = -0.1$. (a) $|\Psi|_{max}$ versus $T = t$; (b) the soliton position versus t.

tion, caused by the radiation, follows from the numerical solution of Eq. (1). For the parameters used in Fig. 2, the results following from this solution are presented in Fig. 3. One finds that the mean value of $|\Psi|_{max} = u_0(t)$, shown in Fig. 3(a), decreases logarithmically, similar to what was found for the case $\alpha_1 = \alpha_2 = 0$ [25,26]. Analyzing the soliton position [Fig. 3(b)] one can find that the soliton velocity $V(t)$ increases from $V(0) = 0$ to $V(138) \approx 0.29$, i.e., the soliton is *accelerating* and the function $V(t)$ increases (also logarithmically). Now, using $\Lambda(0) \approx 0.98$, $\Lambda(138) \approx 0.85$ and Eqs. (47) and (44), we have $\lambda(0) \approx 1.4$, $\lambda(138) \approx 1.28$. Therefore, the soliton width $\Delta = \sqrt{a_2}/\lambda$ increases from $\Delta(0) \approx 0.71$ to $\Delta(138) \approx 0.99$, i.e., the radiating soliton is widening with time. All that can be considered as a numerical confirmation of analytical results obtained in Appendix B from the conservation laws, in particular that

$$\text{sgn}\frac{dV}{dt} = -\text{sgn}\,k = \text{sgn}\,U, \tag{64}$$

which means that the soliton is accelerating in the direction of the group velocity of resonant radiation.

V. SPECIAL CASE $\alpha_1 = 6\alpha_3$

The coefficient q in Eq. (9) disappears at

$$K = 1/\alpha_1. \tag{65}$$

Substituting this in Eq. (10), we have $a_2 = 1 - 6\alpha_3/\alpha_1$. Therefore, at condition (3) the coefficient a_2 also vanishes and Eq. (9) takes the form

$$\partial_t\psi + 6\alpha_3|\psi|^2\partial_x\psi + \alpha_2\psi\partial_x|\psi|^2 + \alpha_3\partial_x^3\psi = 0, \tag{66}$$

which is related to Eq. (1) by a Galilean transformations (5) and (8) with

$$V = \frac{1}{12\alpha_3}, \quad K = \frac{1}{6\alpha_3}, \quad \Omega = \frac{1}{108\alpha_3^2}. \tag{67}$$

Consider a particular solution of Eq. (66)

$$\psi(x,t) = e^{i\theta}\zeta(x,t), \tag{68}$$

where $\theta = \text{const}$ and θ, $\zeta(x,t)$ are real. Then Eq. (66) is reduced to the MKdV equation

$$\partial_t\zeta + 2(3\alpha_3 + \alpha_2)\zeta^2\partial_x\zeta + \alpha_3\partial_x^3\zeta = 0. \tag{69}$$

It is completely integrable and, in particular, has exact N-soliton solutions [22] if $\alpha_2 \neq -3\alpha_3 = -(1/2)\alpha_1$ [cf. Eq. (2b)]. From them, using Eq. (68) and Galilean transformation with parameters (67), we one can find N-soliton solutions of Eq. (1) at $\alpha_1 = 6\alpha_3$. For one-soliton solution we have

$$\psi_s = a\,\text{sech}[b(x - \alpha_3 b^2 t)]e^{i\theta}, \tag{70}$$

where a and b are connected by means of Eq. (2b). This expression, together with Eqs. (5) and (67), leads to the Potasek-Tabor soliton, described by Eqs. (2a)–(2e) with $\kappa = K = 1/6\alpha_3$ ($\alpha_3 \neq 0$). Therefore the N-soliton solutions of Eq. (1), $\Psi_s^N(X,T)$, at $T \rightarrow \pm\infty$, are composed of the Potasek-Tabor solitons.

If, in addition to condition (3), $\alpha_2 = 0$ (Hirota case [4]), we arrive at the complex MKdV equation

$$\partial_t\psi + 6\alpha_3|\psi|^2\partial_x\psi + \alpha_3\partial_x^3\psi = 0. \tag{71}$$

The soliton solution to this equation has the form

$$\psi_s(x,t) = a\,\text{sech}[a(x - ct)]\exp[i(px - \sigma t + \theta)] \tag{72}$$

with arbitrary p and

$$c = -3\alpha_3 p^2 + \alpha_3 a^2, \quad \sigma = -\alpha_3 p^3 + 3\alpha_3 p a^2 \tag{73}$$

[cf. Eq. (70)]. Then

$$\Psi_s(X,T) = a\,\text{sech}[a(X - V_s T)]\exp[i(\kappa X - \omega T + \theta)], \tag{74}$$

where

$$V_s = V + c, \quad \kappa = K + p, \quad \omega = \sigma + \Omega + pV. \tag{75}$$

Therefore now κ is arbitrary and $V_s(\kappa)$ and $\omega(\kappa)$ coincide with Eqs. (2c) and (2d), respectively. This means that Eqs. (74) and (75) indeed describe the Hirota solitons, mentioned in Sec. II A, and Eq. (1) in Hirota case definitely has complex N-soliton solutions. The system of Hirota solitons (especially with $p \neq 0$) seem to be rather interesting objects for
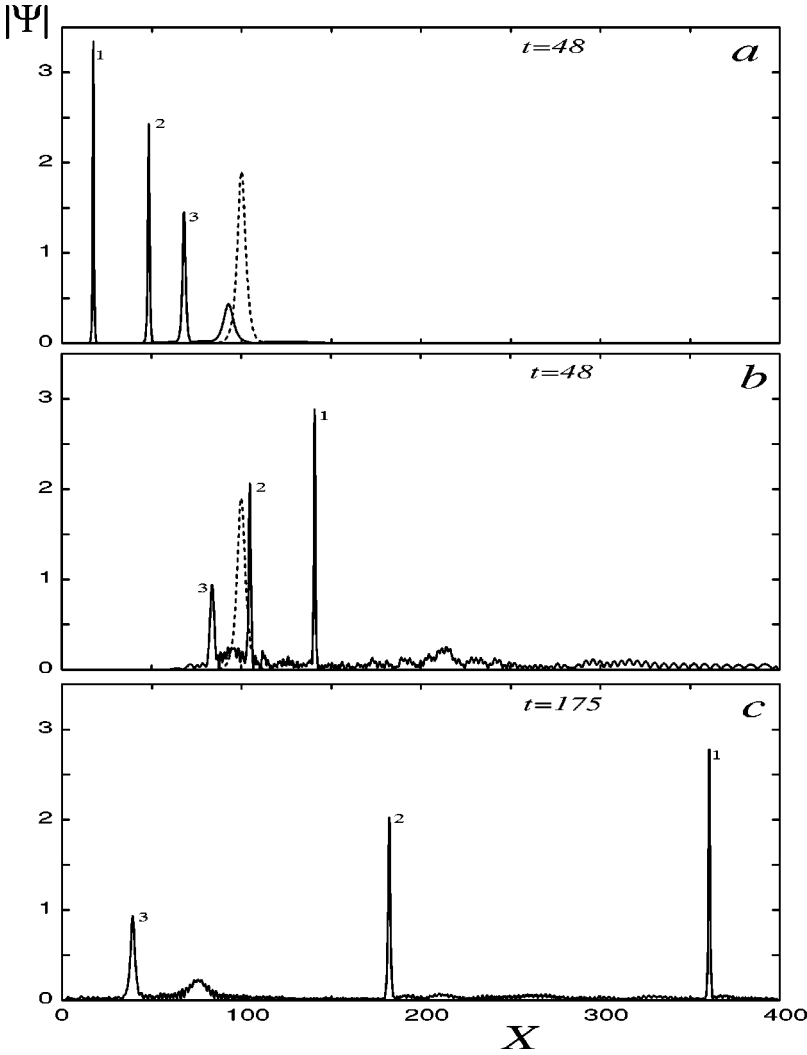
FIG. 4. Development of the initial pulse (76) with $A=1.9$, $C=0$, $X_0=100$ (dashed line). (a) $\alpha_1=-0.5$, $\alpha_2=0$, $\alpha_3=0$, $t=48$, (b) $\alpha_1=-0.5$, $\alpha_2=0$, $\alpha_3=-0.1$, $t=48$, (c) $\alpha_1=-0.5$, $\alpha_2=0$, $\alpha_3=-0.1$, $t=175$.

the soliton theory. Some numerical simulations, demonstrating generation of robust complex Hirota solitons from initial pulses, are described elsewhere [29]. We continue further studies in this field.

As for Eq. (66), it may not be, generally, integrable; one can only assert that it has N-soliton solutions at any $\alpha_2\neq-(1/2)\alpha_1$. Below, we call Eq. (66) general complex MKdV equation. The Painlevé test [21] applied to Eq. (66) shows that it has the Painlevé property if $\alpha_2=3\alpha_3$, i.e., $6\alpha_3=\alpha_1=2\alpha_2$. This is just the integrability condition for Eq. (1) found by Sasa and Satsuma [5]. These conclusions are in agreement with those following from the Painlevé test of Eq. (1) [28,23].

VI. PULSE EVOLUTION AT $\alpha_1\neq6\alpha_3$, $\alpha_2=0$

Here, we report on the numerical solutions of Eq. (1) in general case. First we take, as initial condition, the pulse

$$\Psi(X,0)=A\,\text{sech}\left[\frac{1}{2}(X-X_0)\right]\exp[iC(X-X_0)] \quad (76)$$

with $A=1.9$, $C=0$ and $X_0=100$ and assume that

$$\alpha_1=-0.5, \quad \alpha_3=0.1. \quad (77)$$

The behavior of the solution at these parameters is shown in Fig. 4, where the case $\alpha_3=0$ (with $\alpha_1=-0.5$) is also presented for comparison. In the latter case, the initial pulse splits into four solitons of the form (33) and (35)–(38), with $a_2=1$ and moving to the left [Fig. 4(a)]. On the other hand, in case (77) the initial pulse splits into three *radiating* solitons. Two of them propagate to the right and the smallest one, to the left.

The radiated wave trains propagate to the right with the group velocities larger than the soliton velocities [Figs. 4(b) and 4(c)]; this is in agreement with Eq. (60). The time dependence of the soliton coordinates is shown in Fig. 5. At $\alpha_3=0$, the soliton velocities are constant. At $\alpha_3=-0.1$, the solitons are accelerating in *positive* direction, which agrees with Eq. (64). The Fourier spectra for both cases, $\alpha_3=0$ and $\alpha_3=-0.1$, are shown in Fig. 6. The spectrum at $\alpha_3=0$ exhibits no resonant radiation [Fig. 6(a)] while at $\alpha_3=-0.1$ we see three distinct resonant peaks with negative κ, which are the wave numbers of the resonant radiation emitted by the solitons in the "laboratory" frame [Fig. 6(b)]. The difference between the wave numbers follows from Eq. (20) which is valid, as we have seen, both for embedded and radiating
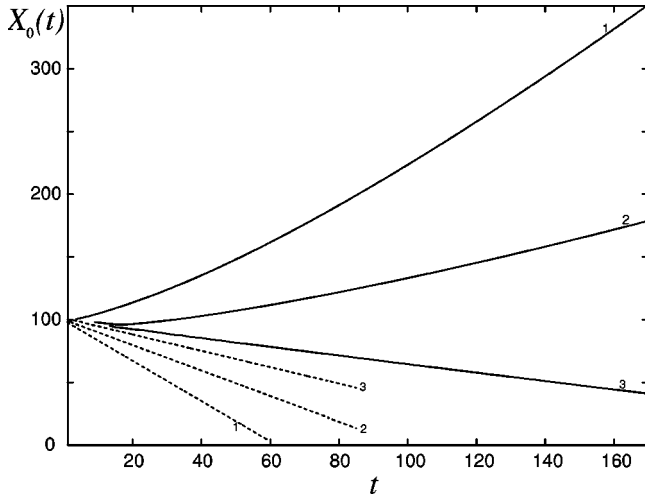
FIG. 5. Plots of $X_0(t)$ for three largest solitons shown in Fig. 8. Dashed line: $\alpha_1 = -0.5$, $\alpha_2 = 0$, $\alpha_3 = 0$; solid line: $\alpha_1 = -0.5$, $\alpha_2 = 0$, $\alpha_3 = -0.1$.

solitons. As far as the solitons have different velocities and amplitudes (the latter are determined by the soliton parameter Λ), they have different wave numbers because κ, being a root of Eq. (20), depends on the soliton velocity and amplitude.

An important difference between the two cases, $\alpha_3 = 0$ and $\alpha_3 \neq 0$, is seen in Figs. 7 and 8. In the first case, the average soliton amplitudes have constant limits at $t \to \infty$
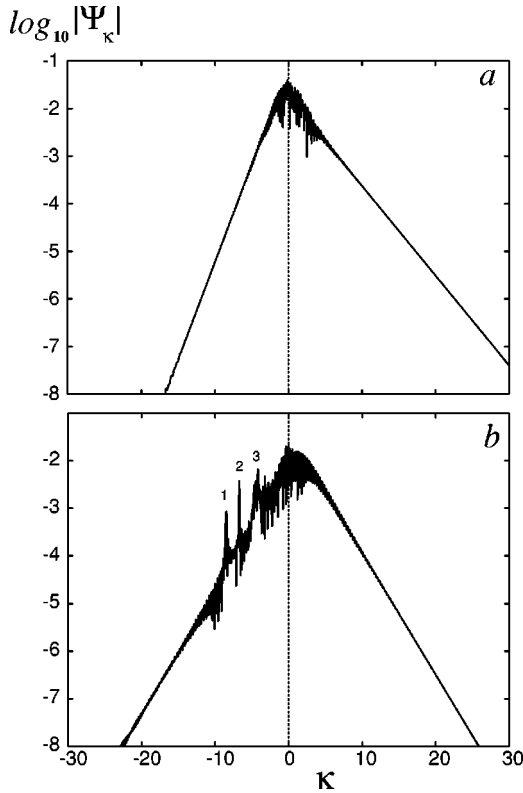
FIG. 6. Fourier spectra of the solutions shown in Fig. 4; (a) $\alpha_1 = -0.5$, $\alpha_2 = 0$, $\alpha_3 = 0$; $t = 48$ (b) $\alpha_1 = -0.5$, $\alpha_2 = 0$, $\alpha_3 = -0.1$; $t = 175$. Here Ψ_κ is the Fourier transform of $\Psi(X)$.
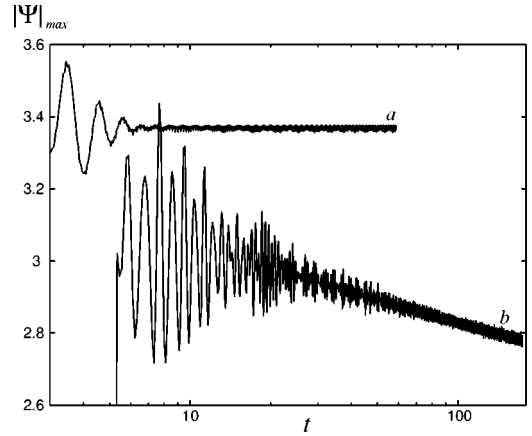

FIG. 7. The amplitude of the first soliton versus time. (a) $\alpha_3 = 0$, (b) $\alpha_3 = -0.1$.

while in the second case they must slowly decrease because of the soliton radiation.

In the aforegoing, we studied the case when $\alpha_1 \alpha_3 \geq 0$. Now let us consider $\alpha_1 \alpha_3 \leq 0$. We take

$$\alpha_1 = -0.6, \quad \alpha_3 = 0.1, \tag{78}$$

and initial condition (76) with $C = 1/2$, $X_0 = 850$. The solution at $T = 370$ is shown in Fig. 9. We see a pulse with radiation on both its sides. An analysis shows that on the left hand side there is the resonantly generated radiation [in agreement with Eq. (60), where now $\alpha_3 > 0$, $k > 0$, $U < 0$). On the right-hand side, there is a radiation composed of the harmonics of continuous spectrum; it satisfies the linearized Eq. (1) and has been emitted in the transient period of time. The spectral distribution is shown in Fig. 10. One can see two spectral maximums at positive wave numbers. The narrow one corresponds to the resonant radiation, while the broader peak is composed of the continuous spectrum. Its structure can be understood from the dispersion equation

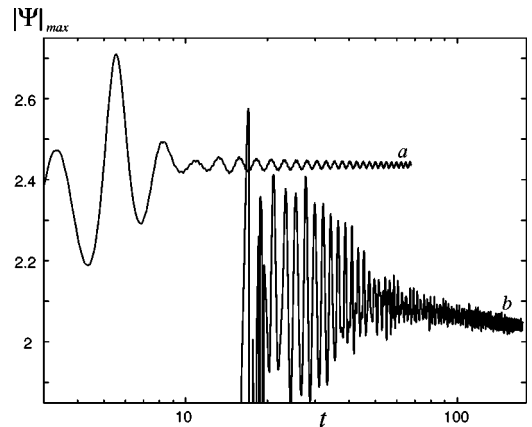$$\omega = (1/2)k^2 - \alpha_3 k^3 \tag{79a}$$

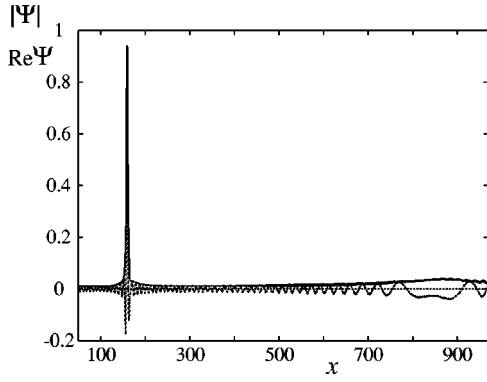FIG. 8. The amplitude of the second soliton versus time. (a) $\alpha_3 = 0$, (b) $\alpha_3 = -0.1$.

FIG. 9. The RRS at parameters $\alpha_1 = -0.6, \alpha_3 = 0.1$. Full line: $|\Psi|$, dotted line: Re Ψ.

and the corresponding expression for the group velocity of continuous spectrum

$$V_g(k) = k - 3\alpha_3 k^2. \tag{79b}$$

From this we see that, at $\alpha_3 > 0$, the continuous radiation on the right-hand side of the pulse is composed from

$$0 < k \leq k_0 = 1/6\alpha_3, \tag{79c}$$

where $V_g(k_0) = \max V_g(k)$. As far as k_0 is less than the wave number of resonant radiation, approximately given by Eq. (50) (note that in our case, according to Eq. (45), $a_2 > 1$), one can see why the peak of continuous spectra is less than κ of resonant radiation. All this shows that the pulse in Fig. 9 is nothing but RRS. The time behavior of its amplitude is shown in Fig. 11; qualitatively, it is similar to Fig. 3(a).

It is reasonable to compare these results with the case $\alpha_1 = -0.6$, $\alpha_3 = 0$, at the same initial condition. Then we have two regular solitons, propagating to the right. The soliton positions versus time for both cases are shown in Fig. 12. Note a very small acceleration of RRS in the direction of group velocity (which is now negative).

VII. CONCLUSIONS

We have considered soliton and quasisoliton solutions of Eq. (1) and their relationship. Solutions (2), describing regu-
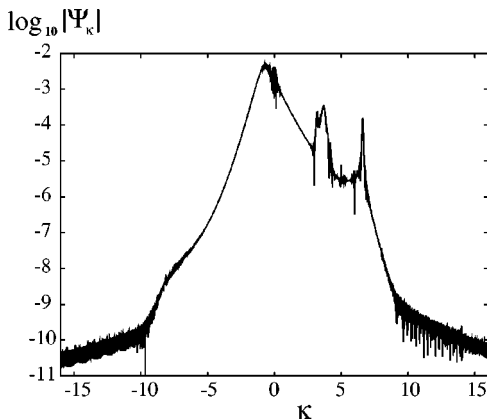

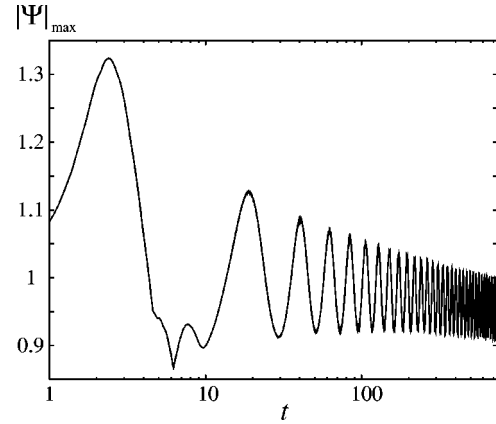FIG. 10. Spectral distribution at $\alpha_1 = -0.6, \alpha_3 = 0.1$.

FIG. 11. Soliton amplitude versus time at $\alpha_1 = -0.6, \alpha_3 = 0.1$.

lar solitons, degenerate at $\alpha_3 \rightarrow 0$; this shows that they exist due a balance between nonlinear terms and linear third-order dispersion. On the other hand the quasisolitons (embedded and resonantly radiating) turn at $\alpha_3 \rightarrow 0$ into the regular soliton solutions of Eq. (1) without the third derivative term. Apart from that, at $\alpha_2 = 0$, the regular solitons exist only in the special case $\alpha_1 = 6\alpha_3$.

The resonantly radiating solitons (RRS) are nonsteady; the amplitudes of their radiation at small α_3 are exponentially small and so their parameters change logarithmically slow in this case. Only such quasisteady solitons have sufficiently large lifetimes to be of physical significance. The embedded solitons (ES), which are steady structures consisting of pulses embedded into plane waves (wings), have close connection with RRS, similar to other systems. The corresponding analytical treatment in Sec. III is supplemented by numerical simulations with the cutoff operation (Sec. IV); it is demonstrated that it leads to the transformation of ES into RRS that radiates in the direction of the radiation group velocity. Just after the cutoff, the amplitude, velocity, and wave number of the radiated wave train coincide with those of wings; marching in time, we have seen that the amplitude decreases, the soliton velocity increases and the wave num-
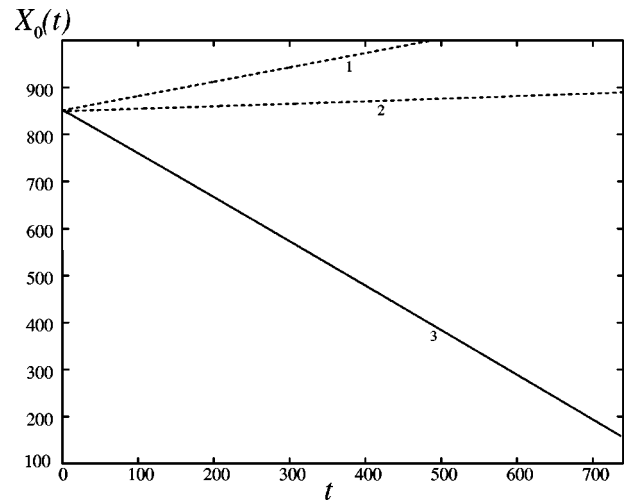

FIG. 12. Soliton positions versus time for $\alpha_1 = -0.6, \alpha_3 = 0$ (1,2) and, $\alpha_1 = -0.6, \alpha_3 = 0.1$ (3).

ber changes according to Eqs. (30) and (31). This is in agreement with conservation laws (Appendix B).

In Sec. V we have investigated a special case $\alpha_1 = 6\alpha_3$, interesting from a theoretical point of view. Then the quasisolitons, ES and RRS, do not exist and Eq. (1) can be reduced, by means of Galilean transformation, to the complex MKdV equation. It turns into two integrable cases: at $\alpha_2 = 0$ (Hirota equation) and at $\alpha_2 = 3\alpha_3$ (Sasa-Satsuma equation). At other values of α_2 it seems to be nonintegrable, despite that it has N-soliton solutions.

Presumably, in the nonlinear *processes* only regular solitons and RRS may be of the physical significance. From Eq. (2b) it follows, however, that the amplitude of regular soliton vanishes at $\alpha_3 \rightarrow 0$, while for the RRS it remains finite. Therefore one should expect that at small α_3, the RRS are more important in the nonlinear evolution. (Small α_3 is the most interesting case from physical point of view because the third derivative term is in fact the result of an expansion.) In Sec. VI we show how RRS are emerging from initial disturbances. This indicates that the RRS are important physical objects playing a significant role in the nonlinear dynamics.

ACKNOWLEDGMENT

APPENDIX A: MODULATIONAL INSTABILITY OF PLANE WAVE, ACCORDING TO EQ. (1)

Equation (1) has exact plane wave solution

$$\Psi = A \exp(i\kappa X - i\omega T). \qquad (A1)$$

Substituting Eq. (A1) into (1), we have

$$\omega = \frac{1}{2}\kappa^2 - (1 - \alpha_1 \kappa)A^2 - \alpha_3 \kappa^3. \qquad (A2)$$

Substituting a slightly perturbed wave (A1)

$$\Psi = A(1 - \chi)\exp(i\kappa X - i\omega T), \qquad (A3)$$

into Eq. (1), we have

$$i\chi_T + \frac{1}{2}(1 - 6\alpha_3 K)\chi_{XX} + i(K + \alpha_1 A^2 - 3\alpha_3 K^2)\chi_X$$

$$+ (1 - \alpha_1 \kappa)(\chi + \chi^*)A^2 + i\alpha_2(\chi_X + \chi_X^*)A^2. \qquad (A4)$$

Writing $\chi = u + iw$ and assuming that

$$(u,w) \approx \exp(ipX - irT).$$

we obtain dispersion equation, which is convenient to write in the form

$$\Gamma^2 - 2\alpha_2 kA^2\Gamma - \frac{1}{4}(1 - 6\alpha_3 K)k^2[(1 - 6\alpha_3 K)k^2$$

$$- 4(1 - \alpha_1 K)A^2] = 0, \qquad (A5)$$

where

$$\Gamma = r + \alpha_3 p^3 - (\kappa - 3\alpha_3 \kappa^2 + \alpha_1 A^2)p. \qquad (A6)$$

Thus, at real p, $\text{Im}\,\Gamma = \text{Im}\,r$ and the stability condition is

$$(1 - 6\alpha_3 \kappa)^2 p^2 \geqslant 4A^2[(1 - \alpha_1 \kappa)(1 - 6\alpha_3 \kappa) - \alpha_2^2 A^2].$$
$$(A7)$$

Unlike the plane wave solution of the regular NLS, now the plane wave can be stable at any p, if

$$(1 - \alpha_1 \kappa)(1 - 6\alpha_3 \kappa) \leqslant \alpha_2^2 A^2. \qquad (A8)$$

At $\alpha_2 = 0$ this is possible at

$$\frac{1}{\alpha_1} \leqslant \kappa \leqslant \frac{1}{6\alpha_3} \quad (6\alpha_3 < \alpha_1) \qquad (A9a)$$

$$\frac{1}{6\alpha_3} \leqslant \kappa \leqslant \frac{1}{\alpha_1} \quad (\alpha_1 < 6\alpha_3). \qquad (A9b)$$

Applying the stability criterion to the wings of embedded solitons, where $\kappa \approx 1/2\alpha_3$, we see that this may satisfy condition (A9b); then one can expect that the wings are stable. We should also take into account only $p > L^{-1}$, where L is the period in the numerical scheme; this relaxes the limitations following from the stability criterion.

APPENDIX B: INVESTIGATION OF THE SOLITON EVOLUTION BY MEANS OF THE INTEGRALS OF MOTION

First, we present a general analysis of conserved integrals N, P, H. Substituting Eq. (5) into expressions (12), (14), and (15) we have after simple algebra

$$N = \int_{\infty}^{\infty} |\psi(x,t)|^2 dx, \qquad (B1)$$

$$P = KN + \frac{1}{2}i\int_{\infty}^{\infty}(\psi\partial_x\psi^* - \psi^*\partial_x\psi)dx, \qquad (B2)$$

where $\psi(x,t)$ satisfies Eq. (9).

To have a convenient expression for H, we substitute in Eq. (15) $\alpha_3\partial_x^3\Psi$ and $\alpha_3\partial_x^3\Psi^*$ from Eq. (1), to obtain

$$H = \frac{i}{2}\int_{\infty}^{\infty}dX(\Psi^*\partial_T\Psi - \Psi\partial_T\Psi^*) + \frac{1}{2}\int_{\infty}^{\infty}dX|\Psi|^4$$

$$+ \frac{i}{4}\alpha_1\int_{\infty}^{\infty}dX|\Psi|^2(\Psi^*\partial_X\Psi - \Psi\partial_X\Psi^*).$$

Then using the Galilei transformation in the form (24) and taking into account that at large t

$$\partial_t \approx i(\lambda^2/2)\psi,$$

we arrive at the following asymptotic expression:

$$H \approx \left(\Omega - KV - \frac{1}{2}\lambda^2 \right) N + PV + \frac{1}{2}q \int_\infty^\infty |\psi|^4 dx$$

$$- \frac{1}{2} i \alpha_1 \int_\infty^\infty |\psi|^2 (\psi \partial_x \psi^* - \psi^* \partial_x \psi) dx. \qquad (B3)$$

Substituting Eqs. (25) and (32) into Eq. (B1), we have at large t (cf. Refs. [25,26]),

$$N \approx N_s + N_r, \qquad (B4)$$

where

$$N_s = \int_\infty^\infty |u_s(x,t)|^2 dx, \quad N_r = \int_\infty^\infty |\eta(x,t)|^2 dx \qquad (B5)$$

are contributions from the soliton and the radiation. Using Eq. (35) we have

$$N_s = \frac{2a_2}{\alpha_1} \arctan\left(\frac{\alpha_1 \lambda}{\sqrt{a_2 q}} \right) \qquad (B6)$$

and, at large t,

$$N_r \approx |f|^2 |U| t \qquad (B7)$$

where f is given by Eq. (52) or (55). Evidently, $|f|^2$ does not depend on x. Then from the conservation of N it follows

$$\frac{d}{dt}\left[\frac{2a_2}{\alpha_1} \arctan\left(\frac{\alpha_1 \lambda}{\sqrt{a_2 q}} \right) \right] \approx -|f|^2 |U|. \qquad (B8)$$

In a similar way, from Eq. (B2) and the conservation of P we have the following asymptotic equation at large t

$$N\frac{dK}{dt} + \frac{d}{dt}\int_\infty^\infty u_s^2(x)\partial_x \psi_s(x) dx + k|f|^2|U| \approx 0. \qquad (B9)$$

From Eq. (36) at $\alpha_2 = 0$, we have

$$\partial_x \psi_s(x) = -\frac{\alpha_1}{2a_2} u_s^2(x). \qquad (B10)$$

Taking into account that

$$\int_\infty^\infty u_s^4(x) dx = \frac{2a_2 q}{\alpha_1}\left(\frac{2\sqrt{a_2}\lambda}{q} - N_s \right), \qquad (B11)$$

we transform Eq. (B9) to the form

$$N\frac{dK}{dt} - \frac{d}{dt}\left[\frac{q}{\alpha_1}\left(\frac{2\sqrt{a_2}\lambda}{q} - N_s \right) \right] + k|f|^2|U| \approx 0. \qquad (B12)$$

Now we turn to Eq. (B3). After differentiation over t and simple calculations we obtain

$$P\frac{dV}{dt} - \left(\lambda\frac{d\lambda}{dt} + a_2 K\frac{dK}{dt} \right) N$$

$$= -\frac{d}{dt}\left[\frac{1}{2}q\int_\infty^\infty |\psi|^4 dx \right.$$

$$\left. + \frac{i}{4}\alpha_1 \int_\infty^\infty |\psi|^2 (\psi^* \partial_x \psi - \psi \partial_x \psi^*) dx \right]$$

$$= -\frac{d}{dt}\left[\frac{1}{2}q\int_\infty^\infty |\psi_s|^4 dx \right.$$

$$\left. + \frac{i}{4}\alpha_1 \int_\infty^\infty |\psi_s|^2 (\psi_s^* \partial_x \psi_s - \psi_s \partial_x \psi_s^*) dx \right]. \qquad (B13)$$

Using

$$\frac{dV}{dt} = a_2 \frac{dK}{dt}, \qquad (B14)$$

we obtain

$$a_2(P - KN)\frac{dK}{dt} - \lambda\frac{d\lambda}{dt}N$$

$$\approx -\frac{d}{dt}\left(\frac{1}{2}q\int_\infty^\infty u_s^4 dx + \frac{\alpha_1^2}{2a_2}\int_\infty^\infty u_s^6 dx \right). \qquad (B15)$$

Let us apply these relations to small α_1 (which is just the case shown in Fig. 3). Assuming that

$$\frac{\alpha_1 \lambda}{\sqrt{a_2 q}} \ll 1, \qquad (B16)$$

we have

$$N_s \approx \frac{2\sqrt{a_2}\lambda}{q}\left(1 - \frac{\alpha_1^2 \lambda^2}{3a_2 q^2} \right). \qquad (B17)$$

Therefore Eq. (B8) is reduced to

$$\frac{d}{dt}\left[\frac{2\sqrt{a_2}\lambda}{q}\left(1 - \frac{\alpha_1^2 \lambda^2}{3a_2 q^2} \right) \right] = -|f|^2|U|. \qquad (B18)$$

In the same approximation, Eq. (B12) takes the form

$$N\frac{dK}{dt} \approx -k|f|^2|U| + \frac{2\alpha_1}{3}\frac{d}{dt}\left(\frac{\lambda^3}{\sqrt{a_2}q^2} \right), \qquad (B19)$$

At $\alpha_1 \to 0$, Eqs. (B18) and (B19) turn into equations obtained in Ref. [18]. From Eqs. (B19), (B14), and (60) follows the important qualitative result (64).

Now, consider Eq. (B15). Taking into account Eqs. (B2), (B10), (B11), and (B19) we see that at

$$t \ll \lambda k^{-2}|f|^{-4}U^{-2} \qquad (B20)$$

and small α_1, Eq. (B15) is approximately equivalent to Eq. (B18). Performing calculations similar to those in Ref. [19] and using Eq. (B14), we conclude that the soliton width λ^{-1} and velocity $V(t)$ are changing logarithmically slow. The same holds for the soliton amplitude $u_0(t)$, determined from Eqs. (39) and (37), in agreement with numerical solution of Eq. (1) (see Fig. 3). The characteristic time of the variations of soliton parameters has the same order of magnitude as in Ref. [26], which is much less than the right hand side of Eq. (B20).

If α_1 is not small, the analysis is rather tedious and will not be considered here.

[1] A. Hasegawa and Y. Kodama, *Solitons in Optical Communications* (Oxford University Press, Oxford, 1995).

[2] G. P. Agrawal, *Nonlinear Fiber Optics* (Academic Press, New York, 1995).

[3] M. J. Potasek and M. Tabor, Phys. Lett. A **154**, 449 (1991).

[4] R. Hirota, J. Math. Phys. **14**, 805 (1973).

[5] N. Sasa and J. Satsuma, J. Phys. Soc. Jpn. **60**, 409 (1991).

[6] E. M. Gromov, L. V. Piskunova, and V. V. Tutin, Phys. Lett. A **256**, 153 (1999).

[7] J. Yang, B. A. Malomed, and D. J. Kaup, Phys. Rev. Lett. **83**, 1958 (1999).

[8] P. K. A. Wai, C. R. Menyuk, Y. C. Lee, and H. H. Chen, Opt. Lett. **11**, 464 (1986).

[9] P. K. A. Wai, H. H. Chen, and Y. C. Lee, Phys. Rev. A **41**, 426 (1990).

[10] H. H. Kuehl and C. Y. Zhang, Phys. Fluids B **2**, 889 (1990).

[11] V. I. Karpman, Phys. Rev. E **47**, 2073 (1993).

[12] J. P. Boyd, *Weakly Nonlocal Solitary Waves and Beyond-All-Order Asymptotics* (Kluwer, Dordrecht, 1998).

[13] V. I. Karpman, in *Nonlinearity, Integrability and All That: Twenty Years After NEEDS'79*, edited by M. Boiti, L. Martina, F. Pempinelli, B. Prinari, and G. Soliani (World Scientific, Singapore, 2000), p. 396.

[14] V. I. Karpman, Phys. Rev. E **62**, 5678 (2000).

[15] P. Deeskow, H. Schamel, N. N. Rao, M. Y. Yu, R. K. Varma, and P. K. Shukla, Phys. Fluids **30**, 2703 (1987).

[16] V. I. Karpman and H. Schamel, Phys. Plasmas **4**, 120 (1997); **4**, 2778(E) (1997).

[17] Y. Pomeau, A. Ramani, and B. Grammaticos, Physica D **31**, 127 (1988).

[18] V. I. Karpman, Phys. Lett. A **181**, 211 (1993).

[19] V. I. Karpman, Phys. Lett. A **186**, 300 (1994).

[20] V. I. Karpman, Phys. Rev. Lett. **74**, 2455 (1995).

[21] J. Weiss, M. Tabor, and G. Carnevale, J. Math. Phys. **24**, 522 (1983).

[22] M. A. Ablowitz and H. Segur, *Solitons and the Inverse Scattering Transform* (SIAM, Philadelphia, 1981).

[23] M. Gedalin, T. C. Scott, and Y. B. Band, Phys. Rev. Lett. **78**, 448 (1997).

[24] V. E. Zakharov and E. A. Kuznetsov, Zh. Éksp. Teor. Fiz. **113**, 1892 (1998) [JETP **86**, 1036 (1998)].

[25] V. I. Karpman and A. G. Shagalov, Phys. Lett. A **254**, 319 (1999).

[26] V. I. Karpman, Phys. Lett. A **244**, 397 (1998).

[27] Zhonghao Li, Lu Li, Huipping Tian, and Guosheng Zhou, Phys. Rev. Lett. **84**, 4096 (2000).

[28] K. Porsezian and K. Nakkeeran, Phys. Rev. Lett. **76**, 3955 (1996).

[29] V. I. Karpman, J. J. Rasmussen, and A. G. Shagalov, e-print nlin.SI/0102008 (2001).